AGU100 ADVANCING EARTH AND SPACE SCIENCE

Geophysical Research Letters

RESEARCH LETTER
10.1029/2018GL077511

Key Points:
- Ice-penetrating radar can detect steeply dipping (up to 30-40 degrees) englacial stratigraphy in blue ice areas
- Despite steep basal topography, the Allan Hills likely preserves a continuous ice core record back at least 500 ka and possibly back 1 Ma
- Downstream propagation of stratigraphic anomalies indicates that surface velocities were ~30% of modern values during the last glaciation

Supporting Information:
- Supporting Information S1

Correspondence to:
L. Kehrl,
kehrl@uw.edu

Citation:
Kehrl, L., Conway, H., Holschuh, N., Campbell, S., Kurbatov, A. V., & Spaulding, N. E. (2018). Evaluating the duration and continuity of potential climate records from the Allan Hills Blue Ice Area, East Antarctica. *Geophysical Research Letters*, *45*. https://doi.org/10.1029/2018GL077511

Received 8 FEB 2018
Accepted 30 MAR 2018
Accepted article online 26 APR 2018

Evaluating the Duration and Continuity of Potential Climate Records From the Allan Hills Blue Ice Area, East Antarctica

Laura Kehrl[1,2], Howard Conway[1], Nicholas Holschuh[1], Seth Campbell[1,3], Andrei V. Kurbatov[3,4], and Nicole E. Spaulding[4]

[1]Earth and Space Sciences, University of Washington, Seattle, WA, USA, [2]Polar Science Center, Applied Physics Laboratory, University of Washington, Seattle, WA, USA, [3]School of Earth and Climate Sciences, University of Maine, Orono, ME, USA, [4]Climate Change Institute, University of Maine, Orono, ME, USA

Abstract The current ice core record extends back 800,000 years. Geologic and glaciological evidence suggests that the Allan Hills Blue Ice Area, East Antarctica, may preserve a continuous record that extends further back in time. In this study, we use ice-penetrating radar and existing age constraints to map the internal stratigraphy and age structure of the Allan Hills Main Ice Field. The dated isochrones provide constraints for an ice flow model to estimate the age of ice near the bed. Previous drilling in the region recovered stratigraphically disturbed sections of ice up to 2.7 million years old. Our study identifies a site ~5 km upstream, which likely preserves a continuous record through Marine Isotope Stage 11 with the possibility that the record extends back 1 million years. Such records would provide new insight into the past climate and glacial history of the Ross Sea Sector.

Plain Language Summary Ice cores currently provide detailed, continuous records of Earth's climate and atmosphere over the past 800,000 years. Discrete ice samples with ages up to 2.7 million years have been recovered from the Allan Hills Blue Ice Area, East Antarctica, indicating that the region may preserve a continuous record that extends beyond 800,000 years. In this study, we use ice-penetrating radar and an ice flow model to identify an optimal site for a continuous ice core record from the Allan Hills, which may extend over the last 1 million years. Such a long ice core record would help us better understand the fundamental drivers of Earth's climate.

1. Introduction

Ice cores currently provide detailed, continuous records of Earth's climate and atmosphere over the past 800,000 years (800 ka; EPICA Community Members, 2004; Masson-Delmotte et al., 2010). Lower-resolution climate records from before 800 ka have been obtained from marine sediments (Clark et al., 2006; Lisiecki & Raymo, 2005). Together, these records show that glacial cycles transitioned from a periodicity of 41 to 100 ka between 1200 and 700 ka ago during the mid-Pleistocene transition (MPT). The causes of the MPT remain poorly understood; hypotheses include a long-term decrease in atmospheric carbon dioxide concentrations (Berger et al., 1999), changes in sea ice extent (Tziperman & Gildor, 2003), and the removal of regolith by glacial erosion in the Northern Hemisphere (Clark et al., 2006). Interest in the MPT has fueled the search for an ice core that spans this time interval, which could help elucidate the characteristics of the transition (Fischer et al., 2013; Jouzel & Masson-Delmotte, 2010).

Previous studies have concluded that a continuous, million-year-old ice core record is more likely to be preserved at a site that satisfies certain conditions: (1) it is near an ice divide, where stratigraphically disturbed ice is less likely due to slow flow (van Liefferinge & Pattyn, 2013); (2) there is negligible basal melt, which removes old ice from the bed (Fischer et al., 2013; Parrenin et al., 2017; van Liefferinge & Pattyn, 2013); and (3) there is limited basal relief, as steep basal topography tends to deform basal ice (Fischer et al., 2013). The Allan Hills Blue Ice Area, East Antarctica (Figure 1), is characterized by steep basal topography, seemingly disqualifying it in the search for an old ice core. Yet stratigraphically discrete ice samples as old as 2.7 ± 0.3 million years (Ma) have been recovered from the region (site BIT-58 in Figure 1a; Higgins et al., 2015; Yan et al., 2017), indicating that the region could preserve a continuous, 1-Ma+ paleoclimate record.

In this study, we determine the likely duration and continuity of a potential paleoclimate record from the Allan Hills Blue Ice Area. Blue ice areas form in regions of high winds, where enhanced sublimation and wind erosion cause net ablation (Bintanja, 1999; Sinisalo & Moore, 2010). Net ablation, combined with subglacial

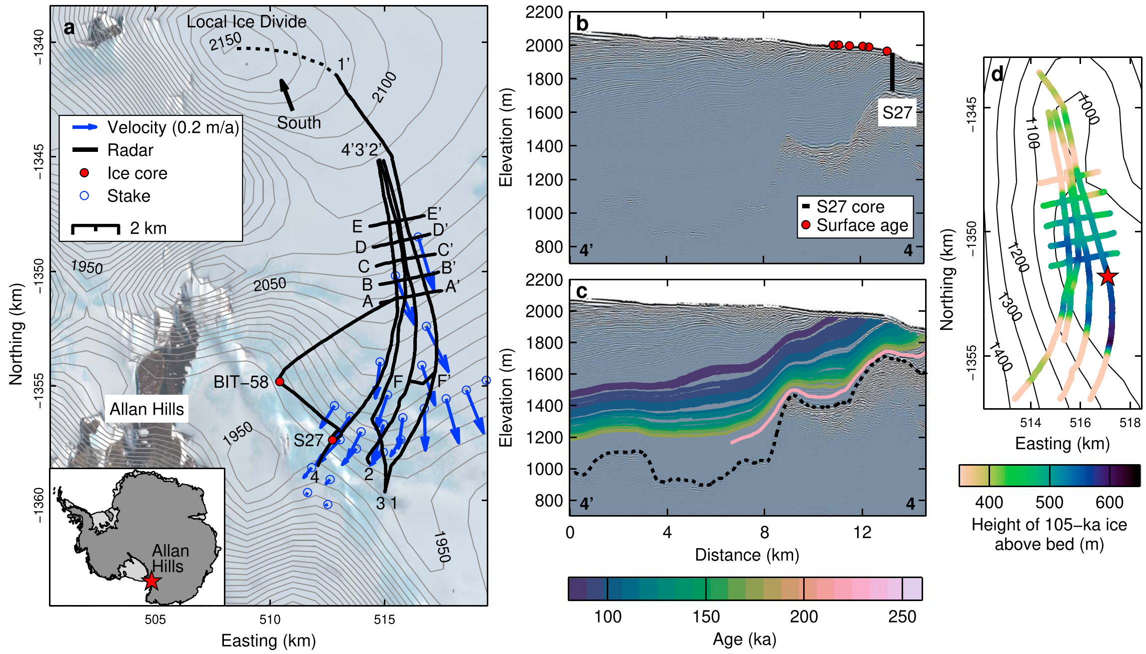

Figure 1. Allan Hills Main Ice Field, East Antarctica. (a) Map showing ice-penetrating radar transects (black curves), ice cores (red circles; Higgins et al., 2015; Spaulding et al., 2013), stakes (blue circles; Spaulding et al., 2012), and surface velocities (blue vectors; Spaulding et al., 2012). Black dashed curve extends Radar Track 1 to the local ice divide. Black arrow indicates south direction. Surface elevation contours from BedMap2 (light gray lines) are shown every 10 m (Fretwell et al., 2013). Background image is a Landsat 8 image from 12 January 2016. Coordinate system is Antarctica Polar Stereographic. (b) Ice-penetrating radar data along Radar Track 4, annotated to show locations of surface ice ages (red circles) as well as ice core S27 (black line), and (c) picked layer ages (colors) and bed (black dashed curve) along Radar Track 4. (d) Height of 105-ka ice above the bed. Bed elevation contours from BedMap2 (black lines) are shown every 100 m. Star indicates the proposed drill site shown in Figure 3b.

topographic barriers, causes the ice to flow toward the surface. These conditions produce steeply dipping englacial layers that outcrop at the surface (Bintanja, 1999; Grinsted et al., 2003; Turney et al., 2013; Whillans & Cassidy, 1983). In the Allan Hills, tephra layers as old as 205 ka are exposed at the surface (Dunbar et al., 1995), and meteorites with ages up to 2.2 Ma have been recovered (Delisle & Sievers, 1991; Nishiizumi et al., 1989).

A continuous ice core record from the Allan Hills could provide insight into the MPT and would offer details about the past climate and stability of the Ross Sea Sector (Spaulding et al., 2013). Only two ice core records from the Ross Sea Sector (Taylor Dome and Talos Dome) currently extend through the penultimate glacial maximum (140 ka; Steig et al., 2000; Stenni et al., 2011), and no record covers Marine Isotope Stage (MIS) 11 (420–360 ka), which is the best known analog for the present-day interglacial period (Howard, 1997; Loutre & Berger, 2003). To determine the likely duration and continuity of a potential ice core record from the Allan Hills Main Ice Field (AH MIF; Figure 1a), we combine an ice flow model (Grinsted et al., 2003) with new ice-penetrating radar data and existing age constraints (Spaulding et al., 2013).

2. Methods

2.1. Ice-Penetrating Radar

Blue ice areas are typically characterized by steeply dipping englacial layers (Bintanja, 1999; Grinsted et al., 2003), but previous studies (Sinisalo et al., 2004; Spaulding et al., 2013; K. Winter et al., 2016), which used very high frequency (50–200 MHz) radar, have only detected these layers to a depth of ~100 m. We used a high-frequency system, with resistively loaded dipole antennas tuned to a center frequency of 7 MHz (wavelength in ice of 24 m), to image englacial layers to a depth of ~900 m in the AH MIF (Figure 1b). To our knowledge, our radar profiles provide the first direct observations of deep englacial stratigraphy in a blue ice area. Radar reflections at this frequency primarily result from electrical conductivity contrasts caused by changes in acidity due to volcanic eruptions or deposition of impurities (Fujita et al., 1999) and can be considered isochrones (layers of equal age). The transmitter and receiver (a digital oscilloscope) were separated by 39 m and towed in-line behind a snowmobile traveling at ~7 km/hr. The receiver was triggered by the airwave from the transmitter. Each radar record consists of 512-stacked waveforms to improve the signal-to-noise ratio. The average distance between records is 2.5 m. We determine the location of each radar record using a Global Positioning System antenna (Garmin 17HVS) mounted 1.5 m behind the receiver; position uncertainties are less than 3 m. Additional data processing includes band-pass filtering and correcting for surface topography. Two-way travel time is converted to depth using wave speeds of 300 m/μs in air and 168.5 m/μs in ice.

2.2. Age Constraints

We manually pick layers of local maximum power return in the radargrams and date those layers using age constraints from horizontal and vertical ice cores near site S27 (Spaulding et al., 2013), which intersects Radar Track 4 (Figures 1a and 1b). Ages from the 225 m, vertical core are linearly interpolated to 13 picked layers that intersect the core; these layers are determined to have ages of 117–243 ka (Spaulding et al., 2013). Where englacial layers intersect the surface upstream of S27, we assign ages from the horizontal core. Near-field radar effects prevent imaging within ~40 m of the surface, so we estimate the point of surface intersection by extrapolating layers using layer slopes calculated below this 40-m threshold. We then linearly interpolate ages from the horizontal ice core to these points of surface intersection, assigning ages spanning 89–108 ka to 15 layers. Figure 1c shows the depth-age scale for Radar Track 4. Finally, we use cross over points between Radar Track 4 and the other tracks to determine layer ages for all radar transects. Figure 1d shows the height of 105-ka ice above the bed for all radar transects. We estimate an age uncertainty of 7 ka for the inferred layer ages (supporting information Text S1).

2.3. Ice Flow Model

To determine the age structure near the bed, we adapt a flowline model that is based on mass conservation (Grinsted et al., 2003). We define x to be the distance along the flowline, y to be the coordinate perpendicular to the flowline, z to be the water equivalent height above the bed, H to be the water equivalent ice thickness, and $\tilde{z} = z/H$ to be the fractional ice thickness. The velocity components of x, y, z, and $\tilde{z}$ are u, v, w, and $\tilde{w}$, respectively. The horizontal velocity is

$$u(\tilde{z}) = f(\tilde{z})u_s \tag{1a}$$

$$v(\tilde{z}) = 0 \tag{1b}$$

and the horizontal velocity gradient is

$$\frac{\partial u}{\partial x} = f(\tilde{z})\frac{\partial u_s}{\partial x} \tag{2a}$$

$$\frac{\partial v}{\partial y} = f(\tilde{z})\frac{\partial v_s}{\partial y}, \tag{2b}$$

where $f(\tilde{z})$ is a shape factor and the subscript s signifies the value at the surface. Following Grinsted et al. (2003), we use

$$f(\tilde{z}) = \frac{\tanh(k\tilde{z})}{\tanh(k)}, \tag{3}$$

which is similar to the shallow-ice approximation assuming no basal sliding (Cuffey & Paterson, 2010). The value of k determines the ice softness and thereby temperature profile used in the model. At the equilibrium line, the steady state temperature profile is linear (Cuffey & Paterson, 2010). Surface velocities are less than 0.5 m/a on both sides of the equilibrium line in the AH MIF (Spaulding et al., 2012), indicating that a linear temperature profile is likely a reasonable assumption for the entire flowline (Grinsted et al., 2003). We set $k = 5$ for a linear temperature profile that decreases from −10 °C at the bed to −30 °C at the ice surface.

The model assumes that the ice thickness remains constant through time. Cosmogenic dating and erosional features indicate that the ice was roughly 100 m thicker in the AH MIF during the Last Glacial Maximum

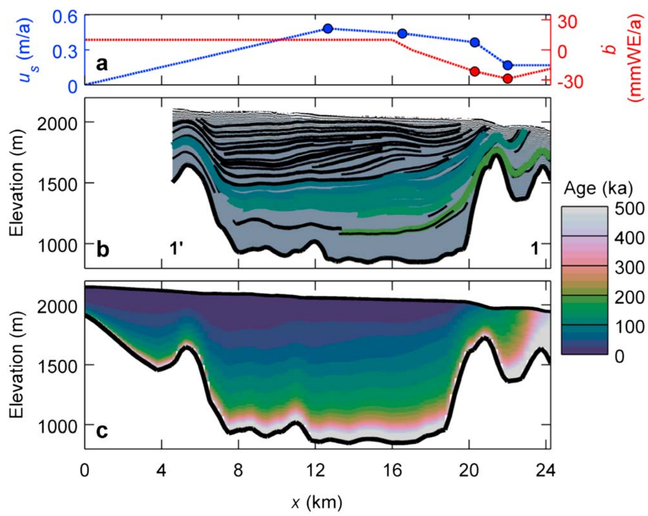

Figure 2. Measured and modeled depth-age scale for Radar Track 1. (a) Present-day surface velocity (u_s) and surface mass balance ($\dot{b}$) linearly interpolated from measured values (colored circles) from Spaulding et al. (2012), (b) measured depth-age scale, and (c) modeled depth-age scale. Black curves in (b) indicate undated, picked layers. For this model run, the present-day accumulation rate ($\dot{b}_o$) is 10-mm water equivalent per year (mmWE/a) and surface velocities decrease to 30% of their present-day values during glacial periods (r = 0.3).

(26–19 ka; Atkins et al., 2002) but likely remained within that range over the last 1 Ma (Yamane et al., 2015). Given this assumption, volume conservation requires

$$\frac{\partial u_s}{\partial x} + \frac{\partial v_s}{\partial y} = \frac{1}{f_m}\left(\frac{\partial u_m}{\partial x} + \frac{\partial v_m}{\partial y}\right) = \frac{\dot{b}}{f_m H}, \tag{4}$$

where $\dot{b}$ is the surface mass balance, with subscript m indicating the mean over the ice column. From mass continuity, we also have

$$\frac{\partial u}{\partial x} + \frac{\partial v}{\partial y} + \frac{\partial w}{\partial z} = 0 \tag{5a}$$

$$\frac{\partial w}{\partial z} = -f(\tilde{z})\left(\frac{\partial u_s}{\partial x} + \frac{\partial v_s}{\partial y}\right). \tag{5b}$$

Equations (5a) and (5b) can be integrated to determine the normalized vertical velocity:

$$\begin{aligned}\tilde{w}(\tilde{z}) &= -\left(\frac{\partial u_s}{\partial x} + \frac{\partial v_s}{\partial y}\right)\int_0^{\tilde{z}} f\left(\tilde{z}'\right) \mathrm{d}\tilde{z}' \\ &= \frac{\left(\frac{\partial u_s}{\partial x} + \frac{\partial v_s}{\partial y}\right)}{-k\tanh(k)}\left(\log\left(\frac{1 + e^{-2k\tilde{z}}}{2}\right) + k\tilde{z}\right).\end{aligned} \tag{6}$$

We combine the horizontal and vertical velocities from equations (1a), (1b), and (6) with a Lagrangian integration scheme to determine particle back trajectories and hence the age structure of the ice (Grinsted et al., 2003).

While more sophisticated models provide better representations of ice flow behavior (e.g., Elmer/Ice; Gagliardini et al., 2013), these models require constraints from detailed observations that are not yet available for the AH MIF. Field observations are sparse (Spaulding et al., 2012), and very little is known about the regional ice flow history over the last 1 to 2 Ma (Atkins et al., 2002; Yamane et al., 2015). The chosen model only requires surface elevation, bed elevation, surface velocity, mass balance, and ice softness parameter (k) along a flowline.

We use Radar Track 1 as the basis for our flowline model because it extends the farthest upstream (Figure 1a). The model domain extends Radar Track 1 to the local ice divide (dashed line in Figure 1a; Spaulding et al., 2012), with the upstream geometry defined by surface and bed elevations from BedMap2 (Fretwell et al., 2013). We use ablation ($\dot{b}$) and surface velocity measurements (u_s) from four stakes installed within 500 m of the flowline from 1997 to 2010 (Figures 1a and 2a; Spaulding et al., 2012). No stake measurements exist within 10 km of the ice divide, so we assume that the velocity decreases linearly to 0 at the divide. Dadic et al. (2015) estimated a long-term accumulation rate of 7.5 mm/a from a shallow ice core, but accumulation rates likely vary spatially and temporally (Bintanja, 1999; Spaulding et al., 2012). For simplicity, we assume a constant, present-day accumulation rate across the accumulation zone, $\dot{b}_o$, which we vary from 5- to 14-mm water equivalent per year (mmWE/a) in 1-mmWE/a increments to assess model sensitivity.

Surface velocity and mass balance likely changed through time. Accumulation rates have been shown to decrease by ~30–50% during glacial periods at other East Antarctica sites (Masson-Delmotte et al., 2010; Watanabe et al., 2003). The change in sublimation rates during glacial periods, however, remains less clear (Bintanja, 1999; Dadic et al., 2013). We assume that snow accumulation rates decrease by 50% during glacial periods and that ablation rates remain constant through time. Surface velocities also likely varied due to changes in surface mass balance, ice temperature, and glacier geometry. To match the age of meteorites exposed at the surface in the Allan Hills Near Western Ice Field, Grinsted et al. (2003) found that present-day velocities must have decreased by 75% during glacial periods. We vary the ratio of glacial to present-day velocities, r, from 0 to 1 in 0.1 increments to assess the sensitivity of our results to this parameter.

Glacial periods are determined using the MIS record from the EPICA Dome C ice core (EPICA Community Members, 2004).

To assess model performance for the 110 different combinations of present-day accumulation rate ($\dot{b}_o$) and the ratio of glacial to present-day velocities (r), we compare the modeled ages to the picked layer ages to determine the model misfit M:

$$M\left(\dot{b}_o, r\right) = \sqrt{\frac{1}{n}\sum_{i=1}^{n}\left(t(i) - t_m(i)\right)^2}, \tag{7}$$

where $t(i)$ is the measured age of layer i at depth $z(i)$ and $t_m(i)$ is its modeled age. The number of layers n varies along the flowline. We calculate model misfit from x = 0 to x = 19 km to avoid biasing our results by high model misfit values in the ablation zone, where we are less interested in the depth-age scale. High model misfit values in the ablation zone do not affect the upstream model performance.

3. Results

Figures 2b and 2c show the measured and modeled depth-age scales for Radar Track 1. We test the sensitivity of the modeled depth-age scale to the present-day accumulation rate ($\dot{b}_o$) and the ratio of glacial to present-day velocities (r). Different combinations of $\dot{b}_o$ and r produce similar model misfit values M of 8–10 ka, as shown in Figure 3a. An increase in $\dot{b}_o$ requires a decrease in r to match the age constraints. The modeled depth-age scale is relatively insensitive to the chosen model parameters. Figure 3b shows the depth-age scale for different best fit combinations of $\dot{b}_o$ and r at x = 16 km (star in Figure 1d; 76° 44.184′S, 159° 4.004′E). At this location, 500-ka ice is 65–70 m above the bed and 1-Ma ice is 31–33 m above the bed for all best fit model combinations. The temporal resolution of the depth-age scale at this location is ~1 ka/m at 250 ka, ~4 ka/m at 500 ka, ~23 ka/m at 750 ka, and ~38 ka/m at 1 Ma. For the rest of the basin, 500-ka ice is 55–70 m above the bed and 1-Ma ice is 25–35 m above the bed (Figure S2).

Given modern observations of accumulation rates and surface velocities (Dadic et al., 2015; Spaulding et al., 2012), our results imply a significant decrease in surface velocity during glacial periods (Figure 3). For a present-day accumulation rate of $\dot{b}_o$=7 mmWE/a, surface velocity must have decreased to 80% of present-day values during glacial periods (r = 0.8); for a present-day accumulation rate of $\dot{b}_o$=10 mmWE/a, velocity must have decreased to 30% of present-day values (r = 0.3).

This decrease in surface velocity is confirmed by the near-surface internal stratigraphy, as shown in Figure 4. Near the surface in Layer 1, a positive thickness anomaly forms after the bedrock bump at x = 7 km (Figures 4a and 4c), perhaps due to enhanced flow convergence or snow accumulation. The thickness anomaly is then buried and advected downstream. By measuring how far this anomaly has moved over a given time interval, we can determine its velocity. The thickness anomaly is 12 km downstream in Layer 5, which is bound by isochrones with ages of 89 and 97 ka, implying a near-surface velocity of ~0.13 m/a, roughly 30% of present-day velocities over the basin (Spaulding et al., 2012). In the flowline model, if we similarly decrease surface velocities to 30% of their present-day values during glacial periods (r = 0.3), the model produces a similar downstream progression in layer thickness (Figures 4b and 4d).

4. Discussion

Ice core drilling in blue ice areas has the potential to replicate and extend the existing ice core record back beyond 800 ka. Low accumulation rates, thin ice cover, and slow flow promote the preservation of old ice in these regions (Spaulding et al., 2012). Together with previous modeling studies in blue ice areas (Grinsted et al., 2003; Moore et al., 2006), our results show that surface velocities were slower in the past, and consequently, ice older than expected from modern ice flow observations is likely present. Blue ice areas, however, are also frequently characterized by complex flow as ice interacts with steep basal topography (Zwinger et al., 2014), which can result in spatial variations in the extent of old ice (Figure 1d) or stratigraphically disturbed ice (Higgins et al., 2015). Hence, even with evidence of very old ice from exposed tephra layers, meteorites, and discrete ice samples (Dunbar et al., 1995; Higgins et al., 2015; Yan et al., 2017), careful site selection is necessary to ensure the retrieval of a continuous, undisturbed ice core record.

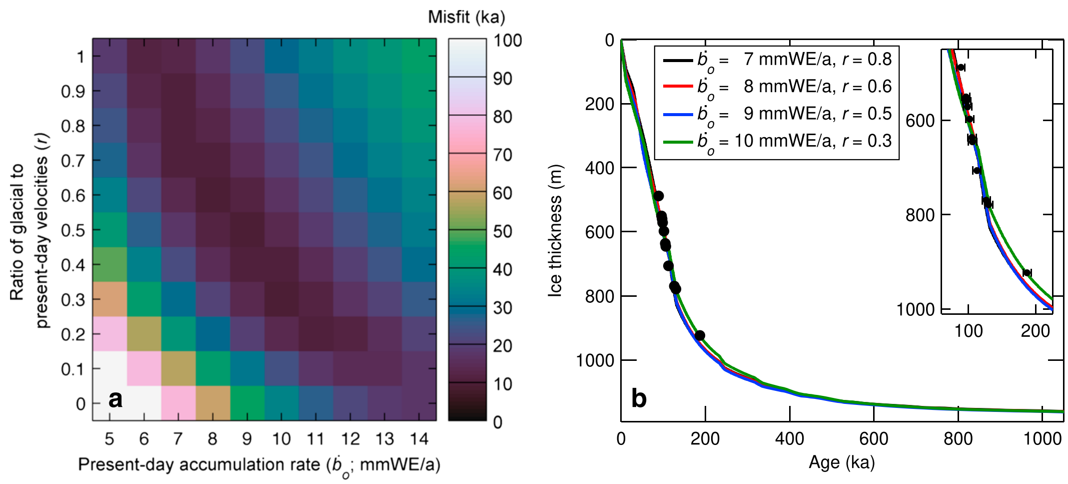

Figure 3. Model sensitivity to the present-day accumulation rate ($\dot{b}_o$) and the ratio of glacial to present-day velocities (r). (a) Model misfit M and (b) measured (points) and modeled (lines) depth-age scales for the proposed drill site at x = 16 km (red star in Figure 1d). mmWE/a = millimeter water equivalent per year.

Our results identify a potential region for a continuous, 1-Ma record from the AH MIF accumulation zone (star in Figure 1d; 76° 44.184′S, 159° 4.004′E). While stratigraphically disturbed ice has been recovered near BIT-58 (Figure 1a; Higgins et al., 2015), our radargrams reveal undisturbed internal stratigraphy to at least 900-m depth in the basin 5–10 km upstream, with no evidence of discontinuities near the surface due to erosion (Figure 1b; K. Winter et al., 2016). Our flow model predicts 1-Ma ice 25–35 m above the bed in this basin. These results indicate that it may be possible to acquire a continuous, 1-Ma ice core record near steep basal topography, which suggests that the current criteria for selecting a 1-Ma+ ice core site should be expanded to include these regions (Fischer et al., 2013; van Liefferinge & Pattyn, 2013). Significant thinning as ice flows out of this basin may help explain the stratigraphically disturbed ice near BIT-58.

The lack of radar-detected layers near the base of the ice makes it difficult to assess whether 1-Ma ice near the bed is disturbed. The oldest radar-detected englacial layer at EPICA Dome C was ~500 ka (A. Winter et al., 2017), but the ice core record was continuous to 800 ka (EPICA Community Members, 2004). Ice retrieved within 60 m of the bed at EPICA Dome C could not be stratigraphically interpreted (Tison et al., 2015). If layers are continuous to 60 m above the bed in the AH MIF, our model predicts a continuous record through ~500 ka. Basal ice in the AH MIF is likely colder that at EPICA Dome C (Tison et al., 2015); Higgins et al. (2015) found no evidence that the bed had chemically or physically altered ice collected 5 m above the

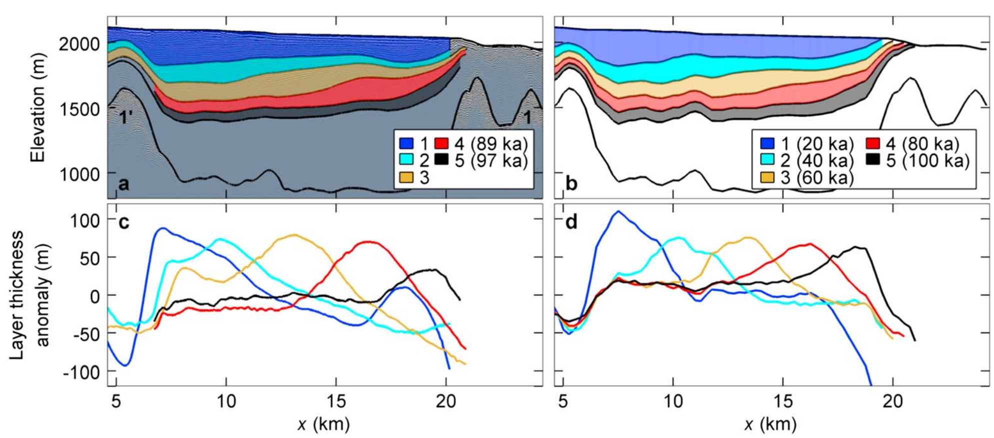

Figure 4. (a) Dated radiostratigraphy and (b) model-derived age structure along Radar Track 1. The thickness of discrete stratigraphic packages seen in the data (shaded in a) and reproduced by the flowline model (shaded in b) has been plotted in (c) and (d) respectively, normalized to the mean package thickness. Panels (c) and (d) highlight the apparent propagation of a thickness anomaly downstream through time, seen in the youngest layers at x = 7 km. The rate of anomaly propagation, deduced from dated isochrones and validated using the flowline model, implies that surface velocities were 30% of modern observed velocities during the last glacial period.

bed at BIT-58. At Taylor Dome, where basal conditions are more similar to those in the AH MIF, the ice core record was continuous to 24 m above the bed (Steig et al., 2000). If layers are continuous to 24 m above the bed in the AH MIF, then a continuous, 1-Ma ice core record may be preserved.

The temporal resolution of 1-Ma ice in an AH MIF ice core (~38 ka/m) will be less than that from other proposed 1-Ma+ sites where the ice thickness is much greater (e.g., 10 ka/m for 1.5-Ma ice near Dome C in Parrenin et al., 2017). It is difficult to evaluate whether the AH MIF record will have sufficient temporal resolution to resolve 41-ka glacial cycles at 1 Ma (Bereiter et al., 2014; Fischer et al., 2013). However, the emergence of new analytic methods and measurements (e.g., Baggenstos et al., 2017; Bender et al., 2008; Buizert et al., 2014; Higgins et al., 2015; NEEM Community Members, 2013; Yan et al., 2017) is enabling the extraction of paleoclimate records from low-resolution, stratigraphically disturbed ice. Hence, even if the basal section of the AH MIF ice core is stratigraphically disturbed, it may still be possible to untangle the paleoclimate record using these methods.

At the very least, the AH MIF should provide a continuous, high-resolution record through MIS 11. Only three ice core records (Dome Fuji, Vostok, and EPICA Dome C) currently extend through this time interval (EPICA Community Members, 2004; Petit et al., 1999), and none of these records are located in the Ross Sea Sector. An ice core from the AH MIF could help constrain the behavior of the Ross Ice Shelf and West Antarctic Ice Sheet during the closest known analog for the present-day interglacial period (Howard, 1997; Loutre & Berger, 2003).

5. Conclusions

We combined an ice flow model, ice-penetrating radar, and existing age constraints to assess past ice flow in the Allan Hills Main Ice Field. Using the approach outlined above, we found that surface velocities were 30% of modern-day values during the last glacial period, indicating that older ice than expected from modern field observations is likely present. Our results reveal a potential drill site for a continuous, 1-Ma ice core record from the Allan Hills Main Ice Field, with 1-Ma ice 25–35 m above the bed. This site does not meet current criteria used in the search for 1-Ma+ ice core sites, indicating that rugged topography should not disqualify potential ice core sites evaluated in future studies. While 1-Ma ice at this site may be stratigraphically disturbed, the proposed drill site should provide a continuous record through at least MIS 11.

Acknowledgments
We thank the U.S. National Science Foundation (grants PLR-1443260 and -1443461) for supporting this project and the Antarctic Support Contractor, Air National Guard, Kenn Borek Air, and UNAVCO for logistical and field support. L. Kehrl was supported by a National Defense Science and Engineering Graduate Fellowship, and N. Holschuh was supported by NASA grant NNX16AM01G. Radar data are available at the U.S. Antarctica Program Data Center (http://www.usap-dc.org/view/dataset/601005). Stake measurements and age constraints are from Spaulding et al. (2012, 2013). Code for the ice-flow model is available at https://github.com/kehrl/allanhills.

References

Atkins, C. B., Barrett, P. J., & Hicock, S. R. (2002). Cold glaciers erode and deposit: Evidence from Allan Hills, Antarctica. *Geology*, *30*(7), 659–662. https://doi.org/10.1130/0091-7613(2002)030%3C0659:CGEADE%3E2.0.CO;2

Baggenstos, D., Bauska, T. K., Severinghaus, J. P., Lee, J. E., Schaefer, H., Buizert, C., et al. (2017). Atmospheric gas records from Taylor Glacier, Antarctica, reveal ancient ice with ages spanning the entire last glacial cycle. *Climate of the Past*, *13*(7), 943–958. https://doi.org/10.5194/cp-13-943-2017

Bender, M., Sowers, T., & Labeyrie, L. (1994). The Dole effect and its variations during the last 130,000 years as measured in the Vostok ice core. *Global Biogeochemical Cycles*, *8*(3), 363–376. https://doi.org/10.1029/94GB00724

Bender, M. L., Barnett, B., Dreyfus, G., Jouzel, J., & Porcelli, D. (2008). The contemporary degassing rate of ^{40}Ar from the solid Earth. *PNAS*, *105*(24), 8232–8237. https://doi.org/10.1073/pnas.0711679105

Bereiter, B., Fischer, H., Schwander, J., & Stocker, T. F. (2014). Diffusive equilibration of N_2, O_2 and CO_2 mixing ratios in a 1.5-million-years-old ice core. *The Cryosphere*, *8*(1), 245–256. https://doi.org/10.5194/tc-8-245-2014

Berger, A., Li, X. S., & Loutre, M. F. (1999). Modelling Northern Hemisphere ice volume over the last 3 Ma. *Quaternary Science Reviews*, *18*(1), 1–11. https://doi.org/10.1016/S0277-3791(98)00033-X

Bintanja, R. (1999). On the glaciological, meteorological, and climatological significance of Antarctic Blue Ice Areas. *Reviews of Geophysics*, *37*(3), 337–359. https://doi.org/10.1029/1999RG900007

Buizert, C., Baggenstos, D., Jiang, W., Purtschert, R., Petrenko, V. V., Lu, Z. T., et al. (2014). Radiometric ^{81}Kr dating identifies 120,000-year-old ice at Taylor Glacier, Antarctica. *Proceedings of the National Academy of Sciences of the United States of America*, *111*(19), 6876–6881. https://doi.org/10.1073/pnas.1320329111

Cavitte, M. P., Blankenship, D. D., Young, D. A., Schroeder, D. M., Parrenin, F., Lemeur, E., et al. (2016). Deep radiostratigraphy of the East Antarctic plateau: Connecting the Dome C and Vostok ice core sites. *Journal of Glaciology*, *62*(232), 323–334. https://doi.org/10.1017/jog.2016.11

Clark, P. U., Archer, D., Pollard, D., Blum, J. D., Rial, J. A., Brovkin, V., et al. (2006). The middle Pleistocene transition: Characteristics, mechanisms, and implications for long-term changes in atmospheric pCO_2. *Quaternary Science Reviews*, *25*(23-24), 3150–3184. https://doi.org/10.1016/j.quascirev.2006.07.008

Cuffey, K. M., & Paterson, W. S. B. (2010). *The physics of glaciers* (4th ed.). Oxford: Elsevier.

Dadic, R., Mott, R., Lehning, M., Carenzo, M., Anderson, B., & Mackintosh, A. (2013). Sensitivity of turbulent fluxes to wind speed over snow surfaces in different climatic settings. *Advances in Water Resources*, *55*, 178–189. https://doi.org/10.1016/j.advwatres.2012.06.010

Dadic, R., Schneebeli, M., Bertler, N. A. N., Schwikowski, M., & Matzl, M. (2015). Extreme snow metamorphism in the Allan Hills, Antarctica, as an analogue for glacial conditions with implications for stable isotope composition. *Journal of Glaciology*, *61*(230), 1171–1182. https://doi.org/10.3189/2015JoG15J027

Delisle, G., & Sievers, J. (1991). Sub-ice topography and meteorite finds near the Allan Hills and near the Western Ice Field, Victoria Land, Antarctica. *Journal of Geophysical Research*, *96*(E1), 15,577–15,587. https://doi.org/10.1029/91JE01117

Dunbar, N. W., Kyle, P. R., McIntosh, W. C., & Esser, R. P. (1995). Allan Hills, Antarctica: A new source of glacial tephrochronological data. *Antarctic Journal of United States*, *30*(5), 76–78.

EPICA Community Members (2004). Eight glacial cycles from an Antarctic ice core. *Nature*, *429*(6992), 623–628. https://doi.org/10.1038/nature02599

Fischer, H., Severinghaus, J., Brook, E., Wolff, E., Albert, M., Alemany, O., et al. (2013). Where to find 1.5 million yr old ice for the IPICS "Oldest-Ice" ice core. *Climate of the Past*, *9*(6), 2489–2505. https://doi.org/10.5194/cp-9-2489-2013

Fretwell, P., Pritchard, H. D., Vaughan, D. G., Bamber, J. L., Barrand, N. E., Bell, R., et al. (2013). Bedmap2: Improved ice bed, surface and thickness datasets for Antarctica. *The Cryosphere*, *7*(1), 375–393. https://doi.org/10.5194/tc-7-375-2013

Fudge, T. J., Waddington, E. D., Conway, H., Lundin, J. M. D., & Taylor, K. (2014). Interpolation methods for Antarctic ice-core timescales: Application to Byrd, Siple Dome and Law Dome ice cores. *Climate of the Past*, *10*(3), 1195–1209. https://doi.org/10.5194/cp-10-1195-2014

Fujita, S., Maeno, H., Uratsuka, S., Furukawa, T., Mae, S., Fujii, Y., & Watanabe, O. (1999). Nature of radio echo layering in the Antarctic ice sheet detected by a two-frequency experiment. *Journal of Geophysical Research*, *104*(B6), 13,013–13,024. https://doi.org/10.1029/1999JB900034

Gagliardini, O., Zwinger, T., Gillet-Chaulet, F., Durand, G., Favier, L., de Fleurian, B., et al. (2013). Capabilities and performance of Elmer/Ice, a new-generation ice sheet model. *Geoscientific Model Development*, *6*(4), 1299–1318. https://doi.org/10.5194/gmd-6-1299-2013

Grinsted, A., Moore, J., Spikes, V. B., & Sinisalo, A. (2003). Dating Antarctic blue ice areas using a novel ice flow model. *Geophysical Research Letters*, *30*(19), 2005. https://doi.org/10.1029/2003GL017957

Higgins, J. A., Kurbatov, A. V., Spaulding, N. E., Brook, E., Introne, D. S., Chimiak, L. M., et al. (2015). Atmospheric composition 1 million years ago from blue ice in the Allan Hills, Antarctica. *Proceedings of the National Academy of Sciences of the United States of America*, *112*(22), 6887–6891. https://doi.org/10.1073/pnas.1420232112

Howard, W. R. (1997). A warm future in the past. *Nature*, *388*(6641), 418–419. https://doi.org/10.1038/41201

Jouzel, J., & Masson-Delmotte, V. (2010). Deep ice cores: The need for going back in time. *Quaternary Science Reviews*, *29*(27–28), 3683–3689. https://doi.org/10.1016/j.quascirev.2010.10.002

Lisiecki, L. E., & Raymo, M. E. (2005). A Pliocene-Pleistocene stack of 57 globally distributed benthic δ^{18}O records. *Paleoceanography*, *20*, PA1003. https://doi.org/10.1029/2004PA001071

Loutre, M. F., & Berger, A. (2003). Marine Isotope Stage 11 as an analogue for the present interglacial. *Global and Planetary Change*, *36*(3), 209–217. https://doi.org/10.1016/S0921-8181(02)00186-8

Masson-Delmotte, V., Stenni, B., Pol, K., Braconnot, P., Cattani, O., Falourd, S., et al. (2010). EPICA Dome C record of glacial and interglacial intensities. *Quaternary Science Reviews*, *29*(1–2), 113–128. https://doi.org/10.1016/j.quascirev.2009.09.030

Moore, J. C., Nishio, F., Fujita, S., Narita, H., Pasteur, E., Grinsted, A., et al. (2006). Interpreting ancient ice in a shallow ice core from the South Yamato (Antarctica) blue ice area using flow modeling and compositional matching to deep ice cores. *Journal of Geophysical Research*, *111*, D16302. https://doi.org/10.1029/2005JD006343

NEEM Community Members (2013). Eemian interglacial reconstructed from a Greenland folded ice core. *Nature*, *493*(7433), 489–494. https://doi.org/10.1038/nature11789

Nishiizumi, K., Elmore, D., & Kubik, P. W. (1989). Update on terrestrial ages of Antarctic meteorites. *Earth and Planetary Science Letters*, *93*(3–4), 299–313. https://doi.org/10.1016/0012-821X(89)90029-0

Parrenin, F., Cavitte, M. G. P., Blankenship, D. D., Chappellaz, J., Fischer, H., Gagliardini, O., et al. (2017). Is there 1.5 million-year old ice near Dome C, Antarctica? *The Cryosphere*, *11*, 2427–2437. https://doi.org/10.5194/tc-11-2427-2017

Petit, J. R., Jouzel, J., Raynaud, D., Barkov, N. I., Barnola, J. M., Basile, I., et al. (1999). Climate and atmospheric history of the past 420,000 years from the Vostok ice core, Antarctica. *Nature*, *399*(6735), 429–436. https://doi.org/10.1038/20859

Sinisalo, A., Grinsted, A., & Moore, J. (2004). Dynamics of the Scharffenbergbotnen blue-ice area, Dronning Maud Land, Antarctica. *Annals of Glaciology*, *39*, 417–422. https://doi.org/10.3189/172756404781814177

Sinisalo, A., & Moore, J. C. (2010). Antarctic blue ice areas—Towards extracting palaeoclimate information. *Antarctic Science*, *22*(02), 99–115. https://doi.org/10.1017/S0954102009990691

Steig, E. J., Morse, D. L., Waddington, E. D., Stuiver, M., Grootes, P. M., Mayewski, P. A., et al. (2000). Wisconsinan and Holocene climate history from an ice core at Taylor Dome, Western Ross Embayment, Antarctica. *Geografiska Annaler. Series A, Physical Geography*, *82*(2-3), 213–235. https://doi.org/10.1111/j.0435-3676.2000.00122.x

Stenni, B., Buiron, D., Frezzotti, M., Albani, S., Barbante, C., Bard, E., et al. (2011). Expression of the bipolar see-saw in Antarctic climate records during the last deglaciation. *Nature Geoscience*, *4*(1), 46–49. https://doi.org/10.1038/ngeo1026

Spaulding, N. E., Higgins, J. A., Kurbatov, A. V., Bender, M. L., Arcone, S. A., Campbell, S., et al. (2013). Climate archives from 90 to 250 ka in horizontal and vertical ice cores from the Allan Hills Blue Ice Area, Antarctica. *Quaternary Research*, *80*(03), 562–574. https://doi.org/10.1016/j.yqres.2013.07.004

Spaulding, N. E., Spikes, V. B., Hamilton, G. S., Mayewski, P. A., Dunbar, N. W., Harvey, R. P., et al. (2012). Ice motion and mass balance at the Allan Hills blue-ice area, Antarctica, with implications for paleoclimate reconstructions. *Journal of Glaciology*, *58*(208), 399–406. https://doi.org/10.3189/2012JoG11J176

Tison, J. L., de Angelis, M., Littot, G., Wolff, E., Fischer, H., Hansson, M., et al. (2015). Retrieving the paleoclimatic signal from the deeper part of the EPICA Dome C ice core. *The Cryosphere*, *9*(4), 1633–1648. https://doi.org/10.5194/tc-9-1633-2015

Turney, C., Fogwill, C., Van Ommen, T. D., Moy, A. D., Etheridge, D., Rubino, M., et al. (2013). Late Pleistocene and early Holocene change in the Weddell Sea: A new climate record from the Patriot Hills, Ellsworth Mountains, West Antarctica. *Journal of Quaternary Science*, *28*(7), 697–704. https://doi.org/10.1002/jqs.2668

Tziperman, E., & Gildor, H. (2003). On the mid-Pleistocene transition to 100-kyr glacial cycles and the asymmetry between glaciation and deglaciation times. *Paleoceanography*, *18*(1), 1001. https://doi.org/10.1029/2001PA000627

van Liefferinge, B., & Pattyn, F. (2013). Using ice-flow models to evaluate potential sites of million year-old ice in Antarctica. *Climate of the Past*, *9*(5), 2335–2345. https://doi.org/10.5194/cp-9-2335-2013

Watanabe, O., Shoji, H., Satow, K., Motoyama, H., Fujii, Y., Narita, H., & Aoki, S. (2003). Dating of the Dome Fuji, Antarctica deep ice core. *Memoirs of National Institute of Polar Research, Special Issue*, *57*, 25–37.

Whillans, I. M., & Cassidy, W. A. (1983). Catch a falling star: Meteorites and old ice. *Science*, *222*(4619), 55–57. https://doi.org/10.1126/science.222.4619.55

Winter, A., Steinhage, D., Arnold, E. J., Blankenship, D. D., Cavitte, M. G. P., Corr, H. J., et al. (2017). Comparison of measurements from different radio-echo sounding systems and synchronization with the ice core at Dome C, Antarctica. *The Cryosphere*, *11*(1), 653–668. https://doi.org/10.5194/tc-11-653-2017

Winter, K., Woodward, J., Dunning, S. A., Turney, C. S. M., Fogwill, C. J., Hein, A. S., et al. (2016). Assessing the continuity of the blue ice climate record at Patriot Hills, Horseshoe Valley, West Antarctica. *Geophysical Research Letters*, *43*, 2019–2026. https://doi.org/10.1002/2015GL066476

Yamane, M., Yokoyama, Y., Abe-Ouchi, A., Obrochta, S., Saito, F., Moriwaki, K., & Matsuzaki, H. (2015). Exposure age and ice-sheet model constraints on Pliocene East Antarctic ice sheet dynamics. *Nature Communications*, *6*(1), 7016. https://doi.org/10.1038/ncomms8016

Yan, Y., Ng, J., Higgins, J., Kurbatov, A., Clifford, H., Spaulding, N., et al. (2017). 2.7-million-year-old ice from Allan Hills blue ice areas, East Antarctica reveals climate snapshots since early Pleistocene. *Goldschmidt Abstracts*, 4359. Retrieved from https://goldschmidtabstracts.info/abstracts/abstractView?id=2017004920

Zwinger, T., Schäfer, M., Martín, C., & Moore, J. C. (2014). Influence of anisotropy on velocity and age distribution at Scharffenbergbotnen blue ice area. *The Cryosphere*, *8*(2), 607–621. https://doi.org/10.5194/tc-8-607-2014